

GT-SVQ: A Linear-Time Graph Transformer for Node Classification Using Spiking Vector Quantization

Huizhe Zhang¹, Jintang Li², Yuchang Zhu¹, Liang Chen^{1,*} and Zibin Zheng²

¹School of Computer Science and Engineering, Sun Yat-sen University, Guangzhou, China

²School of Software Engineering, Sun Yat-sen University, Zhuhai, China

{zhangzh33, lij255, zhuych27}@mail2.sysu.edu.cn, {chenliang6, zhzhbin}@mail.sysu.edu.cn,

Abstract

Graph Transformers (GTs), which simultaneously integrate message passing and self-attention mechanisms, have achieved promising empirical results in some graph prediction tasks. Although these approaches show the potential of Transformers in capturing long-range graph topology information, issues concerning the quadratic complexity and high computing energy consumption severely limit the scalability of GTs on large-scale graphs. Recently, as brain-inspired neural networks, Spiking Neural Networks (SNNs), facilitate the development of graph representation learning methods with lower computational and storage overhead through the unique event-driven spiking neurons. Inspired by these characteristics, we propose a linear-time Graph Transformer using Spiking Vector Quantization (GT-SVQ) for node classification. GT-SVQ reconstructs codebooks based on rate coding outputs from spiking neurons, and injects the codebooks into self-attention blocks to aggregate global information in linear complexity. Spiking vector quantization effectively alleviates the issues concerning *codebook collapse* and the reliance on complex machinery (distance measure, auxiliary loss, etc.) in previous vector quantization-based graph learning methods. In experiments, we compare GT-SVQ with other state-of-the-art baselines on node classification datasets ranging from small to large. Experimental results show that GT-SVQ has achieved competitive performances on most datasets while maintaining up to **130×** faster inference speed compared to other GTs. Our code is available at <https://github.com/Zhhuizhe/GT-SVQ>¹.

1 Introduction

Graph Transformers (GTs), as emerging graph representation learning paradigms, are proposed for alleviating inherent drawbacks of message passing neural networks like over-smoothing, over-squashing and local structure biases [Oono

and Suzuki, 2019][Topping *et al.*, 2021]. Benefiting from the multi-head attention (MHA) modules, vanilla Transformers adaptively learn the global dependencies in input sequences without considering their distance [Vaswani, 2017]. It also provides a solution for learning new topology among nodes while performing message aggregation on the graph data. Experiments demonstrate the immense potential of Transformers in handling global dependencies for graph data [Rampášek *et al.*, 2022][Bo *et al.*, 2023]. However, there is one critical drawback that Transformer with $O(N^2)$ computation complexity is prohibitive for large-scale graphs. Furthermore, the all-pair similarity matrix leads to an increase in degrees of freedom, which often manifests as the full-size Transformers being highly prone to overfitting. Unlike observations in the field of computer vision or natural language process, previous studies show that eliminating redundant components and embracing a lightweight architecture like linear-time attention can significantly enhance the predictive performances of GTs [Wu *et al.*, 2022][Wu *et al.*, 2024].

Recently, with the development of neuromorphic computing, Spiking Neural Networks (SNNs) are poised to bridge the efficiency gap between elaborate network architectures and computation consumption. The defining feature of a SNN is the brain-like spiking mechanism which converts real-value signals into single-bit, sparse spiking signals based on its event-driven biological neurons. The single-bit nature enables us to adopt more addition operations rather than expensive multiply-and-accumulate operations on the spiking outputs, while the sparsity means spikes are cheap to be stored [Eshraghian *et al.*, 2023]. These delightful characteristics have prompted some studies constructing lightweight graph representation learning frameworks to explore binary spike-based representations on the graph data [Zhu *et al.*, 2022][Li *et al.*, 2023a][Li *et al.*, 2023b]. Previous experiments show that the potentiality of SNNs is still underestimated and underappreciated in the domain of graph representation learning. The role of SNNs in modeling the graph structure and dynamics warrants further investigation.

We conduct preliminary experiments to uncover the role of spiking neurons in message propagation. As depicted in Figure 1, there are three observations: **(a)** Those nodes within the same class tend to be closer in the embedding space by performing message propagation-based models. **(b)** The node embeddings from each propagation step are fed into spiking

*Corresponding author

¹Work in progress

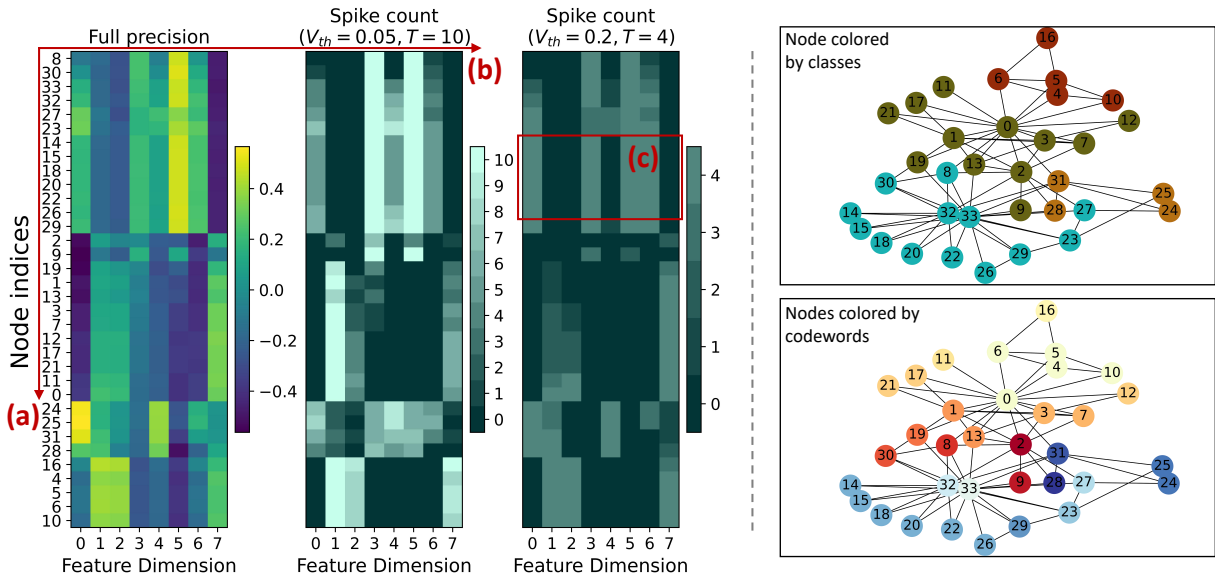


Figure 1: **(left)** Visualization results between full-precision and spike count node embeddings which are respectively generated by a message propagation method and spiking vector quantization on KarateClub. We highlight our observations in red. Notably, though some elements in full-precision embeddings are difficult to differentiate in color, their corresponding values are different. **(right)** Nodes are colored by their raw labels and spike count embeddings (also referred to as codewords) under the setting, $V_{th} = 0.2$ and $T = 4$. It shows that low-precision codewords implicitly group nodes based on learned class label information (e.g., nodes 13, 14, 16 and 24) and structural information (e.g., nodes 14, 15, 18 and 32). More implementation details and visualization results are attached in Appendix A.

neurons to obtain spike count embeddings. It can be considered as generating the low-precision approximations of the original high-precision embeddings. (c) By converting the full-precision embeddings into spike count embeddings, nodes that are close in the original embedding space can be represented by the same low-precision embedding. It projects continuous high-precision representations into discrete low-precision representations, which sparks our curiosity about an interesting research question.

Can we go beyond viewing spiking neurons as simple low-power units, and utilize discrete low-precision node representations to build more efficient Graph Transformers?

Deviating from previous works on efficient GTs, we consider spiking neurons as learnable quantizers, which links the rate coding outputs with the concept of vector quantization (VQ) [Van Den Oord *et al.*, 2017][Mentzer *et al.*, 2023]. We propose GT-SVQ, a linear-time Graph Transformer based on Spiking Vector Quantization for node classification. Specifically, GT-SVQ feeds full-precision embeddings from each message propagation into spiking neurons. Accumulating the spiking outputs to generate spike count embeddings enables nodes to be represented by a finite set of integer embeddings, which we also refer to as codewords. And the self-attention block guided by codewords aggregates the long-range information in linear complexity. It is worth noting that the above conversion from full-precision embeddings to codewords need not explicitly create a codebook. Different from prior works, considering spiking neurons as quantizers to generate codewords effectively addresses the *codebook collapse* defined as the under-usage of the codebook. The contributions of this paper are summarized as follows:

- We conducted an in-depth analysis of spiking neurons in message propagation. Based on the observations, we propose Spiking Vector Quantization (SVQ), which provides a spike-driven learnable codebook paradigm to alleviate inherent issues in existing VQ-based graph learning methods.
- We propose a linear-time Graph Transformer, GT-SVQ, based on the codebook guided self-attention mechanism. GT-SVQ takes the lead in introducing low-precision spike count embeddings from the narrower representation space into Graph Transformers. By calculating attention scores between nodes and node sets grouped by codewords, it effectively captures the long-range information with lower computational overhead.
- We conduct a comprehensive comparison with various state-of-the-art baselines across graphs with various scales. Extensive experiments show that GT-SVQ achieves competitive or even superior predictive performances on most datasets. Besides, GT-SVQ enjoys up to **130x** faster inference speed compared to other GT baselines.

2 Preliminaries

Spiking Neural Network. Although electrophysiological measurements can be accurately calculated by complex conductance-based neurons, the complexity limits their widespread deployment in deep neural networks. A simplified computational unit that retains biological characteristics, known as the Integrate-and-Fire neuron, has been proposed [Salinas and Sejnowski, 2002]. IF neurons have three basic characteristics: **Integrate**, **Fire** and **Reset**. Firstly, the

neuron integrates synaptic inputs from other neurons or external current I to charge its cell membrane. Secondly, when the membrane potential reaches a pre-defined threshold value V_{th} , the neuron fires a spike S . Thirdly, the membrane potential of neuron will be reset to V_{reset} after firing. The neuronal dynamics can be formulated as follows:

$$\textbf{Integrate: } V^t = \Psi(V^{t-1}, I^t) = V^{t-1} + I^t, \quad (1)$$

$$\textbf{Fire: } S^t = \Theta(V^t - V_{th}) = \begin{cases} 1, & V^t - V_{th} \geq 0 \\ 0, & \text{otherwise} \end{cases}, \quad (2)$$

$$\textbf{Reset: } V^t = V^t(1 - S^t) + V_{reset}S^t, \quad (3)$$

where V^t and I^t denote the membrane potential and input current at time step t , respectively. $\Theta(\cdot)$ denotes the fire function, and the Heaviside step function is selected as the fire function in this paper. $\Psi(\cdot)$ is the membrane potential update function. Besides, there are two common variants of IF model, LIF and PLIF [Gerstner *et al.*, 2014][Fang *et al.*, 2021b]. The update function of these neurons can be formalized as follows:

$$\textbf{LIF: } V^t = V^{t-1} + \frac{1}{\tau}(I^t - (V^{t-1} - V_{reset})), \quad (4)$$

$$\textbf{PLIF: } V^t = V^{t-1} + \frac{1}{1 + \exp(-a)}(I^t - (V^{t-1} - V_{reset})), \quad (5)$$

where τ is the membrane time constant and a is a trainable parameter, both of which are used to regulate how fast the membrane potential decays. Except for solely encoding input data into spikes, the rate coding scheme is widely adopted by SNNs to extract meaning from the spiking sequence. In this paper, we transform spiking outputs into spike counts that accumulate S^t over T time steps, $\hat{S} = \sum_{t=0}^T S^t$. Besides, we adopt surrogate gradients during error backpropagation to address the issue of zeros gradients caused by non-differentiable functions [Nefcici *et al.*, 2019]. The surrogate gradient method can be defined as $\Theta'(x) \triangleq \theta'(\alpha x)$, where α represents a smooth factor and $\theta(\cdot)$ represents a surrogate function [Nefcici *et al.*, 2019].

Graph Neural Network. We represent a graph as $\mathcal{G} = (\mathcal{V}, \mathcal{E})$, where \mathcal{V} is a set of nodes and \mathcal{E} is a set of edges among these nodes, $\mathbf{A} \in \mathbb{R}^{N \times N}$ is the adjacency matrix of the graph. Let N denotes the number of nodes. We define the d -dimension nodes' attribute as $\mathbf{X} \in \mathbb{R}^{N \times d}$, which is known as the node feature matrix. For a given node $u \in \mathcal{V}$, GNN aggregates messages from its immediate neighborhood $N(u)$ and updates the node embedding h_u . This message passing process can be formulated as follows:

$$h_u^l = \text{UPDATE}(h_u^{l-1}, \text{AGGREGATE}(h_v^l, \forall v \in N(u))), \quad (6)$$

where h_u^l denotes the updated embedding of node u in the l -th layer, h_u^{l-1} is the embedding from the previous layer. UPDATE and AGGREGATE can be arbitrary differentiable functions.

Self-Attention. As the most prominent component in the Transformer, the self-attention mechanism can be seen as mapping a query vector to a set of key-value vector pairs and calculating a weighted sum of value vectors as outputs. Let nodes' attribute $\mathbf{X} \in \mathbb{R}^{N \times d}$ be the input to a self-attention layer. The attention function is defined as follows:

$$\text{Attn}(\mathbf{X}) = \text{softmax}\left(\frac{\mathbf{Q}\mathbf{K}^T}{\sqrt{d'}}\right)\mathbf{V}, \quad (7)$$

$$\mathbf{Q} = \mathbf{X}\mathbf{W}_q, \mathbf{K} = \mathbf{X}\mathbf{W}_k, \mathbf{V} = \mathbf{X}\mathbf{W}_v, \quad (8)$$

where Query, Key and Value are calculated by learnable projection matrices $W_q, W_k, W_v \in \mathbb{R}^{d \times d'}$. We omit the scalar factor for brevity.

3 GT-SVQ

In this section, we comprehensively detail our approach, GT-SVQ. As depicted in Figure 2, GT-SVQ feeds the graph topology information into the Spiking Vector Quantization (SVQ) to map node embeddings to the spike count embeddings. These codewords will guide the aggregation process in the self-attention module. Besides, auxiliary message passing neural networks as position encoders provide node embeddings containing local positional information to the attention module. In what follows, we detail the implementation of SVQ (Section 3.1). Then, we highlight how the learnable codebook is introduced into self-attention to capture long-range information in the graph (Section 3.2). Finally, we revisit the entire architecture of GT-SVQ one by one (Section 3.3).

3.1 Spiking Vector Quantization

Typically, spiking neural networks are designed for time-varying data. In order to meet the requirement for time-varying data, a common practice in spiking graph neural networks is to repeatedly pass the static graph to spiking neurons at each time step. It inevitably brings high computational and storage overheads. In this work, we collect the node embeddings over T propagation steps as the sequential inputs required for spiking neurons, which effectively reduce additional overheads. Besides, we decompose spike count embeddings accumulated from spiking outputs to dynamically reconstruct codebooks. This avoids the issue of explicitly defining the codebook that contains a large number of unused codewords.

Specifically, (i) we sample a D -dimension random feature matrix $\mathbf{R} \in \mathbb{R}^{N \times D}$ from a uniform distribution, and define a propagation operator \mathbf{P} . Based on \mathbf{P} and \mathbf{R} , we update and collect node embeddings $\mathbf{M} \in \mathbb{R}^{N \times D}$ over T propagation steps, $\mathcal{M} = \{\mathbf{M}^0, \mathbf{M}^1, \dots, \mathbf{M}^T\}$. (ii) Given a SNN, it converts the above sequential node embeddings into spiking outputs $\mathcal{S} = \{\mathbf{S}^0, \mathbf{S}^1, \dots, \mathbf{S}^T\}$, $\mathbf{S} \in \{0, 1\}^{N \times D}$. (iii) The spike count embeddings $\hat{\mathbf{S}} \in \mathbb{Z}^{N \times D}$ are obtained by summing \mathbf{S}^t over T propagation steps. (iv) $\hat{\mathbf{S}}$ can be decomposed into the codebook $\mathbf{C} \in \mathbb{Z}^{B \times D}$ and the one-hot matrix

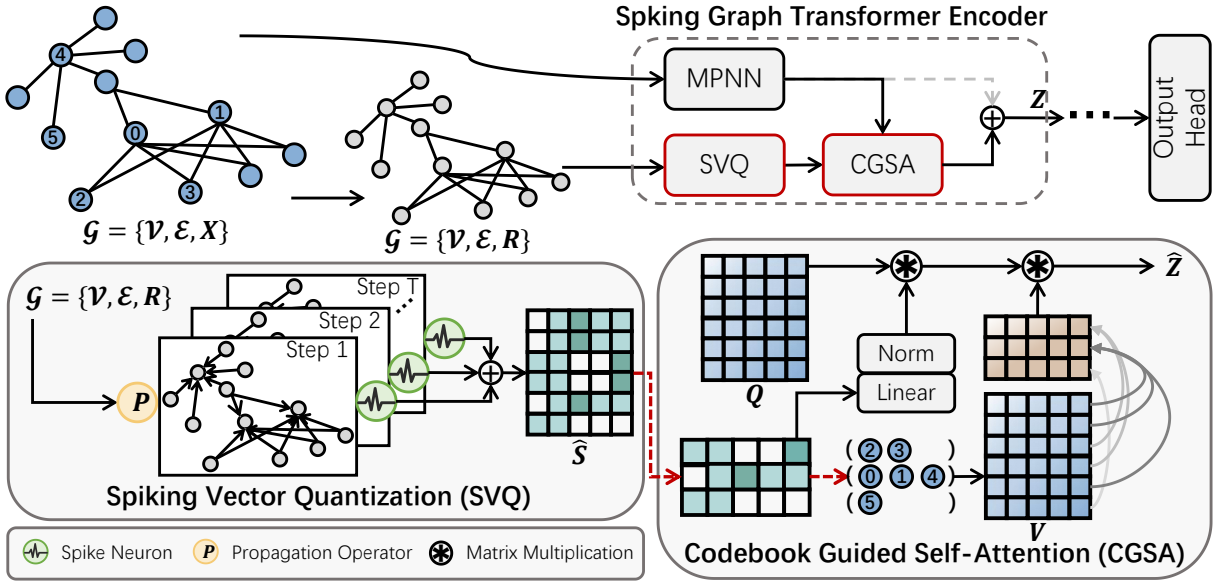


Figure 2: The overview of GT-SVQ. Intuitively, the spiking vector quantization maps nodes to codewords which groups nodes by their structure and feature information. The codebook reconstructed from the spiking count embeddings is fed into the codebook guided self-attention. It assists the self-attention block in calculating attention scores from nodes to grouped node sets in linear time and memory complexity.

$\mathbf{U} \in \{0, 1\}^{N \times B}$. The above processes are defined as:

$$\mathbf{M}^t = \text{Norm}(\mathbf{P}\mathbf{M}^{t-1}), \quad \mathbf{M}^0 = \mathbf{R}, \quad (9)$$

$$\mathbf{s}^t = \Theta(\Psi(V^{t-1}, \mathbf{M}^t) - V_{th}), \quad (10)$$

$$\hat{\mathbf{S}} = \sum_{t=0}^T \mathbf{s}^t, \quad (11)$$

$$\mathbf{U}\mathbf{C} = \hat{\mathbf{S}}, \quad (12)$$

where $\text{Norm}(\cdot)$ is the l_2 normalization, $\Theta(\cdot)$ and $\Phi(\cdot)$ is membrane potential update and fire functions. We choose similar propagation operators presented in previous work [Eliasof *et al.*, 2023]. The codebook \mathbf{C} is created by removing duplicate row vectors in $\hat{\mathbf{S}}$. The one-hot matrix \mathbf{U} can be seen as the indices for where the codewords in $\hat{\mathbf{S}}$ ended up in \mathbf{C} . Hereafter, we will refer to B as the size of the reconstructed codebook.

We define a discrete latent space $\tilde{\mathcal{C}}$ of the spiking count vector $\hat{s} \in \mathbb{Z}^D$, $\forall \hat{s} \in \tilde{\mathcal{C}}$. The size of $\tilde{\mathcal{C}}$ is determined by both the number of propagation steps T and the dimensionality of each random feature D , $|\tilde{\mathcal{C}}| = (T+1)^D$. This is because each dimension can take $T+1$ possible spike counts (considering the case where the total number of spikes is zero) across T time steps. Different from vanilla VQ methods, which explicitly pre-define a codebook containing all latent embedding vectors for lookup, SVQ dynamically maps continuous full-precision embedding to the subset of $\tilde{\mathcal{C}}$ via the SNN. It enables the size of the reconstructed codebook to be much smaller, $B \ll |\tilde{\mathcal{C}}|$, while effectively alleviating the *codebook collapse* problem.

3.2 Codebook Guided Self-Attention

After the spiking vector quantization, we propose a codebook guided self-attention (CGSA) to capture long-range signals in linear complexity. Technically, node embeddings $\mathbf{H} \in \mathbb{R}^{N \times d'}$ generated from auxiliary MPNNs are introduced as Query and Value. We materialize the Key $\hat{\mathbf{K}}$ based on the matrices \mathbf{C} and \mathbf{U} . The attention functions are defined as:

$$\mathbf{Q} = \mathbf{H}\mathbf{W}_q, \quad \mathbf{V} = \mathbf{H}\mathbf{W}_v, \quad (13)$$

$$\mathbf{G} = \text{Norm}(\text{Linear}(\mathbf{C})), \quad (14)$$

$$\hat{\mathbf{K}} = \mathbf{U}\mathbf{G}, \quad (15)$$

$$\hat{\mathbf{Z}} = \text{softmax}(\mathbf{Q}\hat{\mathbf{K}}^T)\mathbf{V}, \quad (16)$$

where d' denotes the dimension of intermediate embeddings. In CGSA, $\hat{\mathbf{K}}$ is calculated based on the matrix multiplication between \mathbf{G} and \mathbf{U} , rather than performing the nearest neighbor look-up on the entire codebook. It avoids the severe reliance on complex components like distance measures or auxiliary losses. Derived from [Lingle, 2023], the attention weights in eq 16 can be further factored:

$$\begin{aligned} \hat{\mathbf{Z}} &= \text{softmax}(\mathbf{Q}\hat{\mathbf{K}}^T)\mathbf{V} \\ &= \text{softmax}(\mathbf{Q}(\mathbf{U}\mathbf{G})^T)\mathbf{V} \\ &= \text{Diag}^{-1}(\exp(\mathbf{Q}\mathbf{C}^T)\mathbf{U}^T\mathbf{1})\exp(\mathbf{Q}\mathbf{C}^T)\mathbf{U}^T\mathbf{V} \end{aligned} \quad (17)$$

where $\mathbf{1} \in \mathbb{R}^N$. $\mathbf{U}^T\mathbf{1} = \{n_b\}_b^B \in \mathbb{Z}^+$ denotes the number of node embeddings in \mathbf{C} mapped to the same codewords. The complexity of CGSA is $O(NBd_v)$, where $B \ll N$. It can be considered that the computational overhead of CGSA grows linearly with the number of nodes. To avoid generating an excessively large codebook in the initial phase of learning, we perform a truncation strategy. We rank n_b from high to low

and select the top B_{max} to generate a truncated codebook, which ensures the training efficiency of our model.

3.3 Overall Framework

As shown in Figure 2, the overview of GT-SVQ includes four modules: SVQ, auxiliary MPNN, CGSA and a classification head (CH). In the SVQ, we construct random features and spiking neurons for each layer. By defining a shared propagation operator, messages among nodes are collected and transformed into spike count embeddings $\hat{\mathbf{S}}$. Then auxiliary MPNNs as encoders generates node embeddings with local positional encodings. In the CGSA, the reconstructed codebook \mathbf{C} , codeword indices \mathbf{U} and node embeddings \mathbf{H} are fed into a linear-time self-attention. Different from the vanilla Transformer, we explicitly inject graph inductive bias by coding global structural information into spike count embeddings. These four parts can be written as follows:

$$\mathbf{U}^l, \mathbf{C}^l = \text{SVQ}^l(\mathbf{A}), \quad (18)$$

$$\mathbf{H}^l = \text{MPNN}^l(\mathbf{Z}^{l-1}, \mathbf{A}), \quad (19)$$

$$\hat{\mathbf{Z}}^l = \text{CGSA}^l(\mathbf{U}^l, \mathbf{C}^l, \mathbf{H}^l), \quad (20)$$

$$\mathbf{Z}^l = \text{Linear}(\hat{\mathbf{Z}}^l) + \mathbf{H}^l, \quad (21)$$

$$\mathbf{Y} = \text{CH}(\mathbf{Z}^L), \quad (22)$$

where L is the number of layers. We choose a simple fully connected layer as the classification head. It has been observed that projection blocks consisting of Multilayer Perceptrons (MLPs) and normalization layers exacerbate the overfitting problem on large-scale graphs for vanilla Transformers. Therefore, we discard redundant projection layers and retain only the self-attention module and the skip-connection structure [He *et al.*, 2016].

4 Experiments

4.1 Comparison with Existing Models

In this section, we conduct the experimental evaluation to show the effectiveness of GT-SVQ on 9 node classification datasets. A head-to-head comparison is conducted with state-of-the-art GNNs and GTs, based on their architectures. As shown in Table 1, these baselines fall into three categories: spike-based methods, Graph Transformer framework and vector quantization-based methods. The hyperparameters search strategy is deployed on both GT-SVQ and other baselines to get the optimal combinations of parameters. We perform all models on each dataset 5 times with different random seeds to report the mean and standard deviation. All experiments are conducted on a single NVIDIA RTX 4090 GPU. More experimental settings are presented in Appendix E.

Overall performance. The experimental results are demonstrated in Table 2. As shown in the table, our method achieves competitive performance on all datasets, which is a significant advancement considering the information loss caused by low-precision spike count embeddings. Furthermore, GT-SVQ achieves predictive performances on par or even better than high-precision GT baselines. **Compared to advanced linear-time GTs, our method shows slight**

Table 1: Comparison of Graph Transformers and Graph Neural Networks w.r.t. required components (**SP**: spike-based, **GT**: Graph Transformer framework, **VQ**: vector quantization-based).

Model	Components		
	SP	GT	VQ
SpikingGCN[Zhu <i>et al.</i> , 2022]	✓	-	-
SpikeNet[Li <i>et al.</i> , 2023a]	✓	-	-
SpikeGCL[Li <i>et al.</i> , 2023b]	✓	-	-
SpikeGT[Sun <i>et al.</i> , 2024]	✓	✓	-
NAGphormer[Chen <i>et al.</i> , 2022]	-	✓	-
NodeFormer[Wu <i>et al.</i> , 2022]	-	✓	-
SGFormer[Wu <i>et al.</i> , 2024]	-	✓	-
GOAT[Kong <i>et al.</i> , 2023]	-	✓	✓
VQGraph[Yang <i>et al.</i> , 2024]	-	-	✓
GT-SVQ	✓	✓	✓

improvements on 7 out of 9 datasets. The results indicate that spiking vector quantization dynamically generates the codebook via the fusion of SNNs and message propagation, and it effectively injects the graph inductive bias into the self-attention block to capture long-range node information. **GT-SVQ outperforms other spike-based baselines on all datasets, which achieves an average improvement of 3.9%.** Constructing the input sequence from propagation steps rather than repeating graphs multiple times endows GT-SVQ with desirable scalability. We also observe that GT-SVQ has comparable performances on two heterophily datasets (particularly Actor), and more discussions about heterophily are provided in Appendix D.

4.2 Characteristics of Spiking Vector Quantization

To elaborately analyze the spiking vector quantization, we conduct a series of experiments on the GT-SVQ. We track the metrics including Codebook Usage and Accuracy to explore the following questions: **(i)** How does the size of latent embedding space affect our model? **(ii)** Is the spiking vector quantization a more efficient VQ alternative?

The influence of $|\tilde{\mathcal{C}}|$. As aforementioned above, the number of propagation steps T and the random feature dimension D determine the size of latent space. In Figure 3, we evaluate the performances of GT-SVQ on Cora and CS datasets under different combinations between D and T . The visualization results show that an excessively small latent space size will severely impair the performances of GT-SVQ. It generally improves accuracy as the latent space size increases. Essentially, $|\tilde{\mathcal{C}}|$ determines the upper bound of information the reconstructed codebook can store. When $|\tilde{\mathcal{C}}|$ is much smaller than the number of nodes, indiscriminately mapping a large number of nodes to the same codeword will bring significant information loss. Besides, we observe the diminishing gains from latent space size scaling, especially on small-scale graphs. We believe that node embeddings merely are transformed into low-precision counterparts rather than being compressed appropriately when feature dimensionality D is too large. The quantization error introduced by spiking neurons will cause performance degradation. The propagation step T correlates with the complexity of spiking patterns. As depicted in Figure 3, it suggests that $T > 6$ may lead to sub-par performance.

Table 2: Classification accuracy(%) on nine datasets. Highlighted are the top **first**, **second** results.

Models	Cora	CiteSeer	PubMed	Co-CS	Co-Physics	Actor	Deezer	arXiv	Products
#nodes	2,708	3,327	19,717	18,333	34,493	7,600	28,281	169,343	2,449,029
#edges	10,556	9,104	88,648	163,788	495,924	30,019	185,504	1,166,243	61,859,140
GCN	81.6 \pm 0.4	71.6 \pm 0.4	78.8 \pm 0.6	92.5 \pm 0.4	95.7 \pm 0.5	30.1 \pm 0.2	62.7 \pm 0.7	70.4 \pm 0.3	75.7 \pm 0.1
GAT	83.0 \pm 0.7	72.1 \pm 1.1	79.0 \pm 0.4	92.3 \pm 0.2	95.4 \pm 0.3	29.8 \pm 0.6	61.7 \pm 0.8	70.6 \pm 0.3	OOM
SGC	80.1 \pm 0.2	71.9 \pm 0.1	78.7 \pm 0.1	90.3 \pm 0.9	93.2 \pm 0.5	27.0 \pm 0.9	62.3 \pm 0.4	68.7 \pm 0.1	74.2 \pm 0.1
VQGraph	81.1 \pm 1.2	74.5\pm1.9	77.1 \pm 3.0	93.3 \pm 0.1	95.0 \pm 0.1	38.7\pm1.6	65.1 \pm 0.2	72.4\pm0.2	78.3\pm0.1
SpikingGCN	79.1 \pm 0.5	62.9 \pm 0.1	78.6 \pm 0.4	92.6 \pm 0.3	94.3 \pm 0.1	26.8 \pm 0.1	58.2 \pm 0.3	55.8 \pm 0.7	OOM
SpikeNet	78.4 \pm 0.7	64.3 \pm 0.8	79.1 \pm 0.5	93.0 \pm 0.1	95.8 \pm 0.7	36.2 \pm 0.9	65.0 \pm 0.2	66.8 \pm 0.1	74.3 \pm 0.4
SpikeGCL	79.8 \pm 0.7	64.9 \pm 0.2	79.4 \pm 0.8	92.8 \pm 0.1	95.2 \pm 0.6	30.3 \pm 0.5	65.0 \pm 1.1	70.9 \pm 0.1	OOM
SpikeGT	82.0 \pm 0.7	70.5 \pm 0.6	71.1 \pm 0.4	92.1 \pm 0.8	95.7 \pm 0.3	36.0 \pm 0.5	65.6 \pm 0.2	70.2 \pm 0.9	OOM
NAGphormer	79.9 \pm 0.1	68.8 \pm 0.2	80.3\pm0.9	93.1 \pm 0.5	95.7 \pm 0.7	33.0 \pm 0.9	64.4 \pm 0.6	70.4 \pm 0.3	73.3 \pm 0.7
GOAT	78.6 \pm 0.5	68.4 \pm 0.7	78.1 \pm 0.5	93.5\pm0.6	95.4 \pm 0.2	37.5 \pm 0.7	65.1 \pm 0.3	72.4\pm0.4	82.0\pm0.4
NodeFormer	82.2 \pm 0.9	72.5 \pm 1.1	79.9 \pm 1.0	92.9 \pm 0.1	95.4 \pm 0.1	36.9 \pm 1.0	66.4\pm0.7	59.9 \pm 0.4	72.9 \pm 0.1
SGFormer	84.5\pm0.8	72.6 \pm 0.2	80.3\pm0.6	91.8 \pm 0.2	95.9\pm0.8	37.9 \pm 1.1	67.1\pm1.1	72.6\pm0.1	72.6 \pm 1.2
GT-SVQ	84.7\pm0.8	74.0\pm0.5	80.6\pm0.4	93.7\pm0.4	96.2\pm0.0	39.1\pm0.2	65.7 \pm 0.1	72.4\pm0.3	74.8 \pm 0.4

Codebook Usage. For exploring the *codebook collapse* problem in VQ-based graph models, we track the fraction of codewords that are used at least once after the training phase. The codebook usages between GT-SVQ and the other VQ-based graph methods are shown in Figure 4. More statistical results are attached in Appendix B. In previous works, the entire discrete latent space is represented as a pre-defined codebook. We select four combinations of D and T ($T = 3/D = 4$, $T = 3/D = 5$, $T = 3/D = 6$, $T = 3/D = 7$) to match the latent space size (2^8 , 2^{10} , 2^{12} , 2^{14}). The results demonstrate that those methods using pre-defined codebooks suffer from the serious issue of *codebook collapse*. As the pre-defined codebook size increases, the codebook usage decreases. For GOAT, the average codebook usages are 10.6% and 8.7% on Cora and CS datasets. The codebook usages in VQGraph are slightly higher, which achieve 16.9% and 29.0%. When the latent space size exceeds 2^{10} , the usages of both methods drop below 50%. It reveals that these VQ-based graph learning methods struggle with efficiently using large pre-defined codebooks. SVQ provides a generative solution, which dynamically selects the subset from a discrete spike count embedding space to reconstruct the codebook. It brings 100% codebook usage. Although the number of used codewords in GT-SVQ will be slightly larger than that of vanilla VQ counterparts in some cases, it is still significantly smaller than the size of pre-defined codebooks. In a nutshell, SVQ efficiently achieves better codebook utilization by implementing vector quantization from the perspective of SNNs.

4.3 Energy Efficiency Analysis

To verify the efficiency of GT-SVQ, we conduct energy efficiency analysis on CS, Physics, ogbn-arxiv and ogbn-products datasets based on the following metrics: the maximum memory usage, inference latency and theoretical energy consumption. The results are shown in Table 3. Besides, we also provide the theoretical energy consumption in the formula and other experimental details in Appendix C.

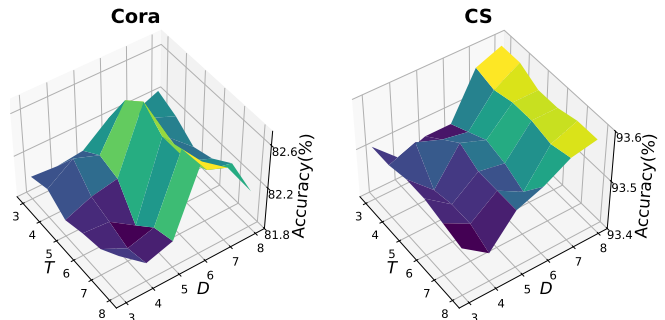


Figure 3: Effects of random feature dimensionality D and propagation step T on Cora and CS.

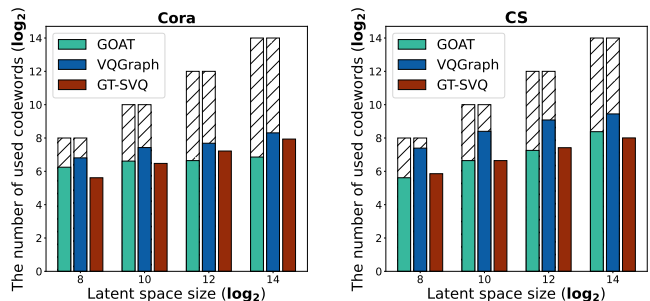


Figure 4: Codebook usage under four different latent space sizes on Cora and CS. The solid-colored bar represents the number of used codewords, while the hatched bar denotes the size of the pre-defined codebook.

The results show that GT-SVQ achieves the lowest inference latency across all datasets. **Compared to other GTs, GT-SVQ with better performance achieves up to 130x lower inference latency.** Most VQ-based methods tend to retrieve and replace node representations with the closest codewords during the inference phase. In SVQ, trained spik-

Table 3: The maximum memory usage (MB), theoretical energy consumption (J) and inference latency (s) of various GT methods. The speedup over average inference latency is underlined.

Datasets	Metrics	NAGphormer	GOAT	NodeFormer	SGFormer	SpikeGT	Avg	GT-SVQ
CS	Latency↓	0.70	5.02	0.05	0.01	0.03	1.16	0.01 ($\times 116$)
	Memory↓	3400	12490	2822	1662	8542	5783	1638
	Energy↓	0.82	1.21	0.21	0.35	0.59	0.64	0.16
Physics	Latency↓	1.79	10.98	0.14	0.02	0.08	2.60	0.02 ($\times 130$)
	Memory↓	13628	22776	7624	2944	16414	12677	3036
	Energy↓	1.86	2.35	0.46	0.78	1.35	1.36	0.37
arXiv	Latency↓	0.78	28.27	1.17	0.10	0.30	6.12	0.08 ($\times 77$)
	Memory↓	10450	21146	11988	6386	22654	14525	7132
	Energy↓	1.12	9.92	0.63	0.57	0.13	2.47	0.18
Products	Latency↓	25.74	2416.84	-	24.34	-	822.30	20.83 ($\times 15$)
	Memory↓	7470	21974	-	934	-	10126	13494
	Energy↓	16.06	143.80	-	8.07	-	55.98	3.69

ing neurons directly convert input features into codewords, which reduces the computational cost brought by retrieval. Integrating the reconstructed codebook in SVQ with linear-time attention modules brings a significant improvement in inference speed. For large-scale graphs with high feature dimensionality, repeating the graph to generate sequential inputs leads to high energy consumption. The results show that the previous spike-based GT consists of spike-driven Transformers and full-precision MPNNs, SpikeGT is hard to manifest its superiority in energy consumption on CS and Physics. Through generating low-dimensional random features and collecting sequential embeddings from propagation steps, **GT-SVQ outperforms another spike-based GT across all datasets with acceptable theoretical energy consumption.**

4.4 Ablation Study

In this section, we conduct ablation studies to explore the influences of different components on predictive performances. To this end, we implement two classic linear-time attention modules (Performer [Choromanski *et al.*, 2020] and Linformer [Wang *et al.*, 2020]), two common spiking neurons (IF and LIF), two normalization algorithms (LayerNorm [Ba *et al.*, 2016] and STFNorm [Xu *et al.*, 2021]) and the vanilla VQ module to construct 7 GT-SVQ variants.

The experimental results are demonstrated in Table 4. Although incorporating extra positional encodings enables Performer and Linformer to handle graph prediction tasks, they struggle to achieve good predictive performance on large-scale graphs like ogbn-arxiv. In GT-SVQ, the CGSA actively introduces the global structure information during attention score calculation. It suggests that developing graph structure-aware Transformers is a promising direction for scaling GTs on large-scale graphs. The choice of spiking neurons also affects the predictive performances of GT-SVQ. PLIF models with learnable membrane time constants and synaptic weights achieve slightly better performances in most cases. These neurons effectively improve the flexibility of SVQ. In addition,

the well-designed normalization algorithm for spiking neurons, STFNorm outperforms the LayerNorm algorithm across all datasets. For spiking graph neural networks, the distribution of spiking node representations and corresponding normalization algorithms lack further exploration. We leave the designs of specific spiking neurons and normalization layers on the graph data for future work.

Table 4: Ablation studies on Pubmed, CS, Physics and ogbn-arxiv datasets. And $+x$ means replacing the original component in GT-SVQ with x .

Models	Pubmed	CS	Physics	ogbn-arxiv
+Performer	80.2 \pm 0.2	93.1 \pm 0.4	95.8 \pm 0.1	71.2 \pm 0.1
+Linformer	79.6 \pm 1.0	92.6 \pm 0.5	95.5 \pm 0.1	65.2 \pm 1.3
+IF	81.6 \pm 1.2	92.8 \pm 0.1	96.0 \pm 0.4	71.0 \pm 0.5
+LIF	79.6 \pm 0.7	92.8 \pm 0.0	96.1 \pm 0.2	72.1 \pm 0.2
+LayerNorm	78.9 \pm 1.3	90.3 \pm 0.6	95.4 \pm 0.4	71.2 \pm 0.2
+STFNorm	82.6\pm0.2	92.3 \pm 0.4	96.5\pm0.5	72.4\pm0.7
+VQ	79.8 \pm 0.4	93.2 \pm 0.3	95.0 \pm 0.4	70.7 \pm 0.7
GT-SVQ	80.6 \pm 0.5	93.7\pm0.4	96.2 \pm 0.0	72.4\pm0.3

5 Conclusion

In this study, we propose GT-SVQ, a linear-time Graph Transformer via spiking vector quantization. We find that message propagation patterns of different nodes can be encoded into the same codewords. Inspired by the observation, GT-SVQ not only considers spiking neurons as the low-power units, but also incorporates SNNs as learnable quantizers into Graph Transformers. It enables GT-SVQ to achieve faster inference speed and better predictive performance. Spike vector quantization which dynamically creates the spike count-based codebook provides a spiking perspective to address issues in current VQ-based graph learning methods. We believe that our work holds great promise from a neuroscientific perspective, and we hope it will inspire further research into more efficient Graph Transformers.

References

- [Alon and Yahav, 2020] Uri Alon and Eran Yahav. On the bottleneck of graph neural networks and its practical implications. *arXiv preprint arXiv:2006.05205*, 2020.
- [Ba et al., 2016] Jimmy Lei Ba, Jamie Ryan Kiros, and Geoffrey E. Hinton. Layer normalization, 2016.
- [Bo et al., 2023] Deyu Bo, Chuan Shi, Lele Wang, and Renjie Liao. Specformer: Spectral graph neural networks meet transformers. *arXiv preprint arXiv:2303.01028*, 2023.
- [Cao et al., 2015] Yongqiang Cao, Yang Chen, and Deepak Khosla. Spiking deep convolutional neural networks for energy-efficient object recognition. *International Journal of Computer Vision*, 113:54–66, 2015.
- [Chen et al., 2022] Jinsong Chen, Kaiyuan Gao, Gaichao Li, and Kun He. Nagphormer: A tokenized graph transformer for node classification in large graphs. *arXiv preprint arXiv:2206.04910*, 2022.
- [Choromanski et al., 2020] Krzysztof Choromanski, Valerii Likhoshershtov, David Dohan, Xingyou Song, Andreea Gane, Tamas Sarlos, Peter Hawkins, Jared Davis, Afroz Mohiuddin, Lukasz Kaiser, et al. Rethinking attention with performers. *arXiv preprint arXiv:2009.14794*, 2020.
- [Diehl et al., 2015] Peter U Diehl, Daniel Neil, Jonathan Binas, Matthew Cook, Shih-Chii Liu, and Michael Pfeiffer. Fast-classifying, high-accuracy spiking deep networks through weight and threshold balancing. In *2015 International joint conference on neural networks (IJCNN)*, pages 1–8. iee, 2015.
- [Eliasof et al., 2023] Moshe Eliasof, Fabrizio Frasca, Beatrice Bevilacqua, Eran Treister, Gal Chechik, and Hagai Maron. Graph positional encoding via random feature propagation. In *International Conference on Machine Learning*, pages 9202–9223. PMLR, 2023.
- [Eshraghian et al., 2023] Jason K Eshraghian, Max Ward, Emre O Neftci, Xinxin Wang, Gregor Lenz, Girish Dwivedi, Mohammed Bennamoun, Doo Seok Jeong, and Wei D Lu. Training spiking neural networks using lessons from deep learning. *Proceedings of the IEEE*, 2023.
- [Fang et al., 2021a] Wei Fang, Zhaofei Yu, Yanqi Chen, Tiejun Huang, Timothée Masquelier, and Yonghong Tian. Deep residual learning in spiking neural networks. *Advances in Neural Information Processing Systems*, 34:21056–21069, 2021.
- [Fang et al., 2021b] Wei Fang, Zhaofei Yu, Yanqi Chen, Timothée Masquelier, Tiejun Huang, and Yonghong Tian. Incorporating learnable membrane time constant to enhance learning of spiking neural networks. In *Proceedings of the IEEE/CVF international conference on computer vision*, pages 2661–2671, 2021.
- [Gerstner et al., 2014] Wulfram Gerstner, Werner M Kistler, Richard Naud, and Liam Paninski. *Neuronal dynamics: From single neurons to networks and models of cognition*. Cambridge University Press, 2014.
- [Hao et al., 2023] Zecheng Hao, Tong Bu, Jianhao Ding, Tiejun Huang, and Zhaofei Yu. Reducing ann-snn conversion error through residual membrane potential. In *Proceedings of the AAAI Conference on Artificial Intelligence*, volume 37, pages 11–21, 2023.
- [He et al., 2016] Kaiming He, Xiangyu Zhang, Shaoqing Ren, and Jian Sun. Deep residual learning for image recognition. In *Proceedings of the IEEE conference on computer vision and pattern recognition*, pages 770–778, 2016.
- [Hu et al., 2020] Weihua Hu, Matthias Fey, Marinka Zitnik, Yuxiao Dong, Hongyu Ren, Bowen Liu, Michele Catasta, and Jure Leskovec. Open graph benchmark: Datasets for machine learning on graphs. *Advances in neural information processing systems*, 33:22118–22133, 2020.
- [Kipf and Welling, 2016] Thomas N Kipf and Max Welling. Semi-supervised classification with graph convolutional networks. *arXiv preprint arXiv:1609.02907*, 2016.
- [Kolesnikov et al., 2022] Alexander Kolesnikov, André Susano Pinto, Lucas Beyer, Xiaohua Zhai, Jeremiah Harmsen, and Neil Houlsby. Uvim: A unified modeling approach for vision with learned guiding codes. *Advances in Neural Information Processing Systems*, 35:26295–26308, 2022.
- [Kong et al., 2023] Kezhi Kong, Jiuhai Chen, John Kirchenbauer, Renkun Ni, C Bayan Bruss, and Tom Goldstein. Goat: A global transformer on large-scale graphs. In *International Conference on Machine Learning*, pages 17375–17390. PMLR, 2023.
- [Li et al., 2018] Qimai Li, Zhichao Han, and Xiao-Ming Wu. Deeper insights into graph convolutional networks for semi-supervised learning. In *Proceedings of the AAAI conference on artificial intelligence*, volume 32, 2018.
- [Li et al., 2023a] Jintang Li, Zhouxin Yu, Zulun Zhu, Liang Chen, Qi Yu, Zibin Zheng, Sheng Tian, Ruofan Wu, and Changhua Meng. Scaling up dynamic graph representation learning via spiking neural networks. In *Proceedings of the AAAI Conference on Artificial Intelligence*, volume 37, pages 8588–8596, 2023.
- [Li et al., 2023b] Jintang Li, Huizhe Zhang, Ruofan Wu, Zulun Zhu, Baokun Wang, Changhua Meng, Zibin Zheng, and Liang Chen. A graph is worth 1-bit spikes: When graph contrastive learning meets spiking neural networks. *arXiv preprint arXiv:2305.19306*, 2023.
- [Li et al., 2024] Wenda Li, Kaixuan Chen, Shunyu Liu, Tongya Zheng, Wenjie Huang, and Mingli Song. Learning a mini-batch graph transformer via two-stage interaction augmentation. *arXiv preprint arXiv:2407.09904*, 2024.
- [Liao and Smidt, 2022] Yi-Lun Liao and Tess Smidt. Equiformer: Equivariant graph attention transformer for 3d atomistic graphs. *arXiv preprint arXiv:2206.11990*, 2022.
- [Lingle, 2023] Lucas D Lingle. Transformer-vq: Linear-time transformers via vector quantization. *arXiv preprint arXiv:2309.16354*, 2023.

- [Ma *et al.*, 2021] Yao Ma, Xiaorui Liu, Neil Shah, and Jiliang Tang. Is homophily a necessity for graph neural networks? *arXiv preprint arXiv:2106.06134*, 2021.
- [Mentzer *et al.*, 2023] Fabian Mentzer, David Minnen, Eirikur Agustsson, and Michael Tschannen. Finite scalar quantization: Vq-vae made simple. *arXiv preprint arXiv:2309.15505*, 2023.
- [Neftci *et al.*, 2019] Emre O Neftci, Hesham Mostafa, and Friedemann Zenke. Surrogate gradient learning in spiking neural networks: Bringing the power of gradient-based optimization to spiking neural networks. *IEEE Signal Processing Magazine*, 36(6):51–63, 2019.
- [Oono and Suzuki, 2019] Kenta Oono and Taiji Suzuki. Graph neural networks exponentially lose expressive power for node classification. *arXiv preprint arXiv:1905.10947*, 2019.
- [Rampášek *et al.*, 2022] Ladislav Rampášek, Michael Galkin, Vijay Prakash Dwivedi, Anh Tuan Luu, Guy Wolf, and Dominique Beaini. Recipe for a general, powerful, scalable graph transformer. *Advances in Neural Information Processing Systems*, 35:14501–14515, 2022.
- [Roy *et al.*, 2019] Kaushik Roy, Akhilesh Jaiswal, and Priyadarshini Panda. Towards spike-based machine intelligence with neuromorphic computing. *Nature*, 575(7784):607–617, 2019.
- [Salinas and Sejnowski, 2002] Emilio Salinas and Terrence J Sejnowski. Integrate-and-fire neurons driven by correlated stochastic input. *Neural computation*, 14(9):2111–2155, 2002.
- [Sen *et al.*, 2008] Prithviraj Sen, Galileo Namata, Mustafa Bilgic, Lise Getoor, Brian Galligher, and Tina Eliassi-Rad. Collective classification in network data. *AI magazine*, 29(3):93–93, 2008.
- [Shchur *et al.*, 2018] Oleksandr Shchur, Maximilian Mumme, Aleksandar Bojchevski, and Stephan Günnemann. Pitfalls of graph neural network evaluation. *arXiv preprint arXiv:1811.05868*, 2018.
- [Shirzad *et al.*, 2023] Hamed Shirzad, Ameya Velingker, Balaji Venkatachalam, Danica J Sutherland, and Ali Kemal Sinop. Exphormer: Sparse transformers for graphs. In *International Conference on Machine Learning*, pages 31613–31632. PMLR, 2023.
- [Sun *et al.*, 2024] Yundong Sun, Dongjie Zhu, Yansong Wang, Zhaoshuo Tian, Ning Cao, and Gregory O’Hared. Spikegraphormer: A high-performance graph transformer with spiking graph attention. *arXiv preprint arXiv:2403.15480*, 2024.
- [Topping *et al.*, 2021] Jake Topping, Francesco Di Giovanni, Benjamin Paul Chamberlain, Xiaowen Dong, and Michael M Bronstein. Understanding over-squashing and bottlenecks on graphs via curvature. *arXiv preprint arXiv:2111.14522*, 2021.
- [Van Den Oord *et al.*, 2017] Aaron Van Den Oord, Oriol Vinyals, et al. Neural discrete representation learning. *Advances in neural information processing systems*, 30, 2017.
- [Vaswani, 2017] A Vaswani. Attention is all you need. *Advances in Neural Information Processing Systems*, 2017.
- [Veličković *et al.*, 2017] Petar Veličković, Guillem Cucurull, Arantxa Casanova, Adriana Romero, Pietro Lio, and Yoshua Bengio. Graph attention networks. *arXiv preprint arXiv:1710.10903*, 2017.
- [Wang *et al.*, 2020] Sinong Wang, Belinda Z Li, Madian Khabsa, Han Fang, and Hao Ma. Linformer: Self-attention with linear complexity. *arXiv preprint arXiv:2006.04768*, 2020.
- [Wu *et al.*, 2019] Felix Wu, Amauri Souza, Tianyi Zhang, Christopher Fifty, Tao Yu, and Kilian Weinberger. Simplifying graph convolutional networks. In *International conference on machine learning*, pages 6861–6871. PMLR, 2019.
- [Wu *et al.*, 2022] Qitian Wu, Wentao Zhao, Zenan Li, David P Wipf, and Junchi Yan. Nodeformer: A scalable graph structure learning transformer for node classification. *Advances in Neural Information Processing Systems*, 35:27387–27401, 2022.
- [Wu *et al.*, 2024] Qitian Wu, Kai Yang, Hengrui Zhang, David Wipf, and Junchi Yan. Sgformer: Single-layer graph transformers with approximation-free linear complexity. *arXiv preprint arXiv:2409.09007*, 2024.
- [Xu *et al.*, 2021] Mingkun Xu, Yujie Wu, Lei Deng, Faqiang Liu, Guoqi Li, and Jing Pei. Exploiting spiking dynamics with spatial-temporal feature normalization in graph learning. *arXiv preprint arXiv:2107.06865*, 2021.
- [Yang *et al.*, 2024] Ling Yang, Ye Tian, Minkai Xu, Zhongyi Liu, Shenda Hong, Wei Qu, Wentao Zhang, CUI Bin, Muhan Zhang, and Jure Leskovec. Vqgraph: Rethinking graph representation space for bridging gnns and mlps. In *The Twelfth International Conference on Learning Representations*, 2024.
- [Yao *et al.*, 2024] Man Yao, Jiakui Hu, Tianxiang Hu, Yifan Xu, Zhaokun Zhou, Yonghong Tian, Bo Xu, and Guoqi Li. Spike-driven transformer v2: Meta spiking neural network architecture inspiring the design of next-generation neuromorphic chips. *arXiv preprint arXiv:2404.03663*, 2024.
- [Zheng *et al.*, 2021] Hanle Zheng, Yujie Wu, Lei Deng, Yifan Hu, and Guoqi Li. Going deeper with directly-trained larger spiking neural networks. In *Proceedings of the AAAI conference on artificial intelligence*, volume 35, pages 11062–11070, 2021.
- [Zhou *et al.*, 2022] Zhaokun Zhou, Yuesheng Zhu, Chao He, Yaowei Wang, Shuicheng Yan, Yonghong Tian, and Li Yuan. Spikformer: When spiking neural network meets transformer. *arXiv preprint arXiv:2209.15425*, 2022.
- [Zhu *et al.*, 2022] Zulun Zhu, Jiaying Peng, Jintang Li, Liang Chen, Qi Yu, and Siqiang Luo. Spiking graph convolutional networks. *arXiv preprint arXiv:2205.02767*, 2022.

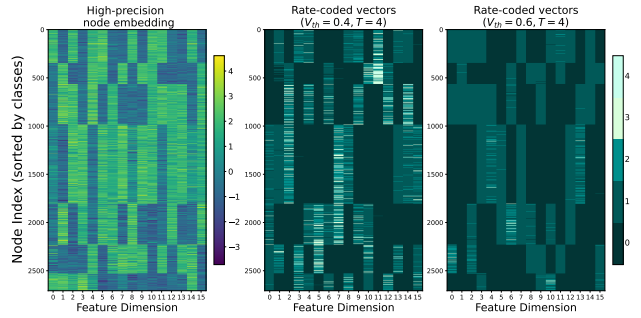
A Visualization Results of SVQ

To better demonstrate our observations, we perform SVQ and a simple message propagation model on the KarateClub dataset. Specifically, for the full-precision message propagation model, the intermediate embeddings across multi-step message propagation are fed into a mean aggregator to generate the node embeddings. The initial node features are sampled from a uniform distribution over the interval $(0, 1)$, and the number of propagation steps is set to 4. For SVQ, the propagation steps are set to 10 and 4 to exhibit the impact of different spiking neuron settings on spike count embeddings. In the preliminary experiments, we observe that **as the number of propagation steps increases, the neighborhood message embeddings of nodes in the same class become increasingly similar**. It implies that we can generate the same representation for different nodes by capturing the dynamics in the propagation process. Benefiting from the powerful coding mechanism of SNNs for sequential data, we fed the above intermediate embeddings into spiking neurons to generate node representations based on spike counts. **different nodes are represented by the same codeword, which means high-precision node embeddings can be encoded into a finite set of codewords from narrower and discrete spike count embedding space.**

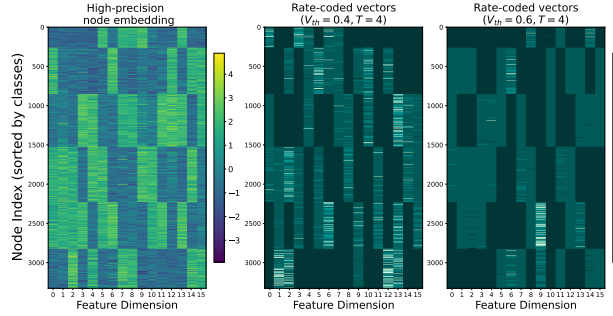
Furthermore, we perform the SVQ and the full-precision message propagation model on Cora, Citeseer and Pubmed datasets. In the implementation, the random features will serve as the initial membrane potential of spiking neurons. SVQ updates node representation by alternating propagation and normalization operations. The adjacency matrix with self-loops and l_2 normalization are selected as the propagation operator and normalization function, respectively. Visualization results are shown in Figure 5. The high-precision node representations (the leftmost plot in each line) can be projected into the finite set of low-precision codewords (the two rightmost plots in each line). Considering iteratively propagated messages as input currents of spiking neurons will generate expressive low-precision node vectors. Additionally, the results reveal **the precision of codewords is governed by spiking neurons with different configurations**. Higher threshold potentials always correspond to lower fire rates or spike counts, which indirectly drives SVQ to generate node representation with lower precision.

B Codebook Usage

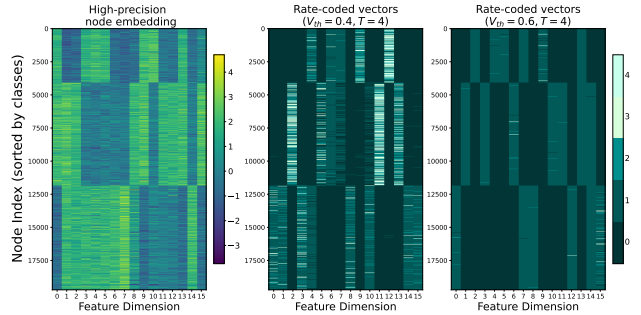
In Table 5, we show the codebook usages and predictive performances of GT-SVQ and VQ-based graph learning baselines on Cora and CS. For VQGraph and GOAT, as the latent space size increases, the number of used codewords continues growing but the codebook usage decreases. GOAT is more sensitive to the latent space size. When the space size is excessively small, GOAT struggles with quantizing the learned node embedding vectors. For the latent space of size 2^8 , GOAT exhibits obvious performance gaps compared with the other two methods on both datasets. In GT-SVQ, the size of the reconstructed codebook B is equal to the number of used codewords. We observe that enlarging the latent space by choosing a larger feature dimensionality D will significantly



(a) The spike count visualization on Cora.



(b) The spike count visualization on Citeseer.



(c) The spike count visualization on Pubmed.

Figure 5: The visualization results of node representations which are decoded in the form of the spike count. The feature dimension is set to 16 and nodes are sorted by their categories. Brighter spots denote higher spike counts.

increase the reconstructed codebook size. Therefore, the feature dimensionality should be decided according to the scale of graph data. As mentioned in Section 3.2, the complexity of CGSA is $O(NBd_v)$. In practice, B may be smaller than the dimensionality of intermediate embeddings. This contributes to the superior inference speed and computational efficiency of CGSA compared to some existing linear-time attention modules.

C Energy Efficiency Analysis

We utilize the maximum memory usage, inference latency and theoretical energy consumption as metrics to comprehensively evaluate the energy efficiency of various GT baselines. Specifically, we record the absolute elapsed running time per test epoch for GT-SVQ and other GT baselines. Notably, following the same settings as previous studies [Wu et

Table 5: Codebook analysis on Cora and CS datasets. For each, we compare GT-SVQ with the other two VQ-based graph models, VQGraph and GOAT. Two metrics are tracked, codebook usage (Usage) and accuracy (ACC).

Models	Latent space size	Cora		CS	
		Usage(%)	ACC(%)	Usage(%)	ACC(%)
VQGraph	2^8	112/256 (43.8)	$81.8_{\pm 1.2}$	168/256 (65.6)	$91.9_{\pm 0.1}$
	2^{10}	172/1024 (16.8)	$81.0_{\pm 1.0}$	338/1024 (33.0)	$92.0_{\pm 0.5}$
	2^{12}	206/4096 (5.0)	$81.4_{\pm 1.1}$	542/4096 (13.2)	$91.8_{\pm 0.4}$
	2^{14}	317/16384 (1.9)	$81.8_{\pm 1.9}$	697/16384 (4.3)	$91.7_{\pm 0.4}$
GOAT	2^8	76/256 (29.7)	$68.4_{\pm 0.6}$	49/256 (19.1)	$56.1_{\pm 3.2}$
	2^{10}	99/1024 (9.7)	$68.3_{\pm 0.9}$	100/1024 (9.8)	$92.2_{\pm 0.3}$
	2^{12}	100/4096 (2.4)	$72.2_{\pm 0.4}$	154/4096 (3.8)	$92.4_{\pm 1.0}$
	2^{14}	116/16384 (0.7)	$78.6_{\pm 0.5}$	333/16384 (2.0)	$92.0_{\pm 0.8}$
GT-SVQ	T=3,D=4	49 (100.0)	$82.0_{\pm 1.0}$	58 (100.0)	$93.4_{\pm 0.4}$
	T=3,D=5	89 (100.0)	$82.0_{\pm 1.7}$	100 (100.0)	$93.4_{\pm 0.3}$
	T=3,D=6	149 (100.0)	$82.2_{\pm 1.2}$	171 (100.0)	$93.5_{\pm 0.3}$
	T=3,D=7	245 (100.0)	$82.1_{\pm 1.2}$	257 (100.0)	$93.6_{\pm 0.8}$

al., 2024], we use the mini-batch partition for training on the ogbn-products dataset.

The theoretical energy consumption estimation is derived from [Yao *et al.*, 2024]. In comparison, we fix some hyper-parameters like the number of layers, the number of heads and the dimension of hidden embeddings for each model. The theoretical energy consumption of GTs during the inference phase is estimated in a straightforward way by counting floating point operations (FLOPs) and synaptic operations (SOPs). The energy cost of GT-SVQ can be formulated as follows:

$$\begin{aligned}
 E &= \sum_{l=1}^L (E_{SVQ} + E_{CGSA} + E_{MPNN} + E_{coding}) + E_{CH} \\
 &= \alpha_s \left(\sum_{l=1}^L \sum_{t=1}^T SP^{l,t}_{SVQ} \right) + \alpha_f \left(\sum_{l=1}^L (FP^{l}_{CGSA} + FP^{l}_{MPNN} \right. \\
 &\quad \left. + FP^{l}_{coding}) + FP_{CH} \right) \quad (23)
 \end{aligned}$$

where α_f and α_s , as scale factors for floating point and synaptic operations, are set to 4.5 and 0.9. FP and SP are denoted as floating point operations and synaptic operations of each layer. $SP^{l,t} = r^{l,t} \times FLOP^{l,t}$, where $r^{l,t}$ is the fire rate of spiking neurons in the l -th layer at the t -th time step. E_{coding} derived from [Zhou *et al.*, 2022] is the energy consumption concerning the conversion between real-valued and spiking presentations in each layer. Notably, we can generate and store codewords corresponding to each node on the neuromorphic hardware. It enables GT-SVQ to maintain the codebook with relatively low energy consumption.

The energy efficiency analysis in table 3 shows that GT-SVQ achieves the highest inference speedup on Physics. As depicted in Figure 6, GT-SVQ has achieved the highest accuracy (96.2%) and the fastest inference speed (21ms) among GT baselines on the Physics dataset. Compared with SVQ, the traditional strategy in VQ-based graph learning methods which measures distances and then replaces embeddings is inefficient. Besides, GT-SVQ achieves faster inference speed, better predictive performance and smaller memory footprint compared to another spike-based GT. We further construct

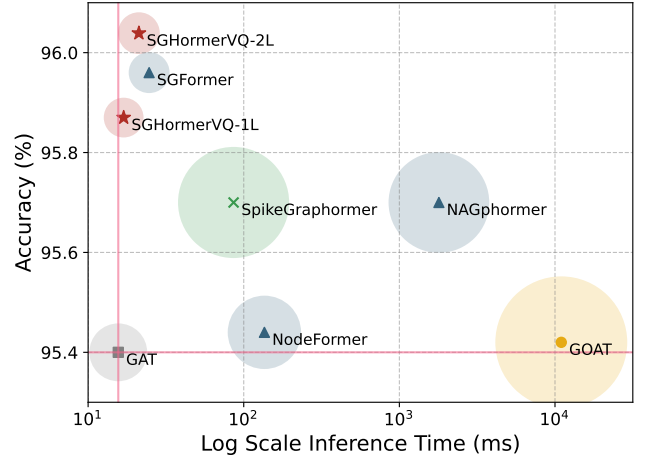


Figure 6: Accuracy versus Inference Time. The size of the circle indicates the maximum memory usage during model training.

the one-layer GT-SVQ. Benefiting from the fusion of SVQ and CGSA, GT-SVQ-1L can rapidly capture local and global graph information while bringing inference speed closer to that of standard GNNs like GAT.

D Revisiting GT-SVQ in the perspective of homophily

There is a popular notion that message propagation-based methods are more suitable for graphs with high-level homophily [Ma *et al.*, 2021]. Therefore, in this section, we conduct a quantitative analysis to investigate whether the homophily of graphs is one of the determining factors on the performance of GT-SVQ. Specifically, we perform the same graph generation strategy on Cora and Citeseer datasets following the previous study [Ma *et al.*, 2021]. Figure 7 shows the influences of different homophily ratios on predictive results, where the homophily ratio is defined as

$\frac{|\{(v,w):(v,w) \in \mathcal{E} \cap y_v = y_w\}|}{|\mathcal{E}|}$. We find that as the homophily ratio decreases, the classification performance initially declines but eventually starts to improve. It is consistent with previous observations [Ma *et al.*, 2021] that the homophily assumption of message passing methods is not accurate. And it implies GT-SVQ may achieve strong performances on certain heterophilic graphs. The results in Table 2 show that GT-SVQ does achieve the best classification accuracy on the Actor dataset compared with other baselines. Empirical results highlight the efficacy of GT-SVQ on both heterophilic and homophilic graphs.

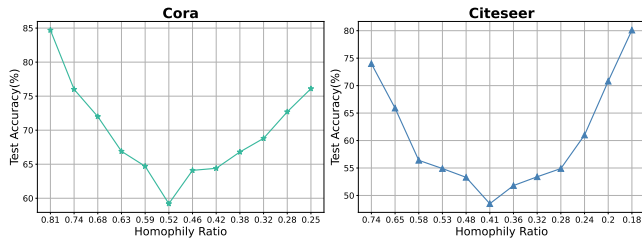


Figure 7: The accuracy of GT-SVQ on synthetic graphs (Cora and Citeseer) with various homophily ratios.

E Experimental Setup

Datasets. We evaluate GT-SVQ on 9 datasets including three citation networks [Sen *et al.*, 2008] (Cora, CiteSeer, PubMed), two co-author networks [Shchur *et al.*, 2018] (Coauthor-CS and Coauthor-Physics), two heterophily networks (Actor and Deezer) and two large-scale graphs (ogbn-arxiv and ogbn-products) from the Open Graph Benchmark (OGB) [Hu *et al.*, 2020]. For citation networks, the data splits adhere to the semi-supervised settings. For co-author networks and heterophily networks, we adopt the same splits in previous studies [Li *et al.*, 2023b][Wu *et al.*, 2024]. For datasets from the OGB, we adopt their own standard splits.

Baselines. To comprehensively evaluate the performance of GT-SVQ, a head-to-head comparison is conducted with state-of-the-art GNNs and GTs, based on their architectures. As shown in Table 1, components in baselines are fall into three categories: spike-based methods (SpikingGCN [Zhu *et al.*, 2022], SpikeNet [Li *et al.*, 2023a], SpikeGCL [Li *et al.*, 2023b], SpikeGT [Sun *et al.*, 2024]), Graph Transformer framework (NAGphormer [Chen *et al.*, 2022], NodeFormer [Wu *et al.*, 2022], SGFormer [Wu *et al.*, 2024], GOAT [Kong *et al.*, 2023]), vector quantization-based methods (VQGraph [Yang *et al.*, 2024]). Besides, three classic graph neural networks (GCN [Kipf and Welling, 2016], GAT [Veličković *et al.*, 2017], SGC [Wu *et al.*, 2019]) are also included in the comparison.

F Related Work

Spiking Neural Network. Inspired by brain-like spiking computational frameworks, Spiking Neural Networks are proposed to address the computing energy consumption challenge. Different from Artificial Neural Networks (ANNs),

neurons in SNNs communicate via binary and sparse spikes. It enables SNNs to reduce the storage overhead of intermediate outputs among layers and utilize more accumulation operations instead of multiply-accumulation operations [Roy *et al.*, 2019]. Some studies motivated by these advantages in energy efficiency have attempted to construct spike-driven neural networks. These networks can be broadly divided into two categories, ANN-to-SNN conversion and direct training framework. For the former, they tend to build a SNN upon a pre-trained ANN. These methods try to minimize information loss during the conversion process by performing scaling/normalizing operations on weights or replacing the activation layers with spiking neurons [Diehl *et al.*, 2015][Cao *et al.*, 2015][Hao *et al.*, 2023]. For the latter, studies try to directly train spike-driven neural networks by introducing surrogate gradient. This approach effectively reduces the strong dependence of SNNs on the number of time steps [Fang *et al.*, 2021a][Zheng *et al.*, 2021].

Graph Transformers. Although graph neural networks (GNNs) have become dominant paradigm cross various graph tasks [Kipf and Welling, 2016][Veličković *et al.*, 2017], the message passing mechanism as the foundations of GNNs has some well-known drawbacks such as over-smoothing, over-squashing and the neglect of long-range information [Li *et al.*, 2018][Alon and Yahav, 2020]. Graph Transformers (GTs), which can differentially aggregate messages over all nodes to alleviate local structure bias, have been developed to overcome above issues. Specifically, methods tend to inject the graph topology information into Transformer variants by introducing auxiliary GNNs or generating positional/structural embeddings from a graph. For some early studies, GTs are proposed to solve small-scale graph-level tasks like molecular property prediction and molecule classification [Rampásek *et al.*, 2022][Liao and Smidt, 2022]. Recently, some methods aimed to enhance GTs’ performance on node-level tasks by constructing mini-batch sampling strategies and lightweight attention modules [Shirzad *et al.*, 2023][Li *et al.*, 2024].

VQ-VAE and Follow-up. To overcome the issue of posterior collapse, [Van Den Oord *et al.*, 2017] develop a discrete latent variational autoencoder (VAE) model called VQ-VAE. Input images are mapped to the embedding space through an encoder. The embeddings are replaced with the nearest pre-defined codebook entries through measuring distances between embeddings and entries. The replaced outputs are then fed into the decoder. It’s worth noting that VQ-VAE utilizes a commitment loss and the straight-through estimator to update the codebook and encoder-decoder modules. In addition, [Kolesnikov *et al.*, 2022] adopted a codebook splitting algorithm to improve codebook usage. [Mentzer *et al.*, 2023] implicitly constructs a finite scalar codebook by quantizing elements of intermediate embeddings to integers. In a nutshell, experiments have shown that VQ-VAE and its variants provide a simpler representation generation schema and an energy-efficient inference framework compared with their quantization-free counterparts.